ELSEVIER

International Journal of Mass Spectrometry 176 (1998) 149–159

International Journal of Mass Spectrometry

Matrix-assisted laser desorption/chemical ionization with reagent ion generation directly from a liquid matrix

K. Breuker, R. Knochenmuss, R. Zenobi*

Department of Chemistry, Swiss Federal Institute of Technology (ETH), Universitätstrasse 16, CH-8092 Zürich, Switzerland

Received 18 December 1997; accepted 26 February 1998

Abstract

Highly concentrated aqueous salt solutions were tested for their ability to serve as a reagent anion source for matrix-assisted laser desorption/chemical ionization (MALD/Cl). It was found that tetrabutylammonium salt/silicon binary matrices yielded abundant deprotonated analyte signals. Moreover, controlled, specific fragmentation of carbohydrates, nucleotides, and peptides was observed, providing useful structural information. The degree of fragmentation was found to depend on the proton affinity of the reagent anion used. (Int J Mass Spectrom 176 (1998) 149–159) © 1998 Elsevier Science B.V.

Keywords: Chemical ionization; Two-phase MALDI

1. Introduction

Chemical ionization mass spectrometry (CIMS), introduced by Munson and Field in 1966 [1], was the first example of a soft gas-phase ionization method, by which the formation of molecular ion species is enhanced relative to the formation of fragment ions. Analytes are ionized in ion-molecule reactions with reagent ions that are generated by electron bombardment of a neutral reagent gas. Typical Cl ion sources operate at 0.5–2.0 torr, with the reagent gas present in at least thousandfold molar excess. This requires pulsed reagent gas introduction or differential pumping in the mass spectrometer. Analyte molecules must be volatile at room temperature or be readily vaporized by heating the sample probe [2]. The technique is not generally applicable because a sufficient amount of intact gas-phase neutral analyte molecules needs to be present in the ion source. This limitation was partially lifted by introduction of laser desorption/chemical ionization (LD/Cl), first reported by Cotter in 1980. The laser was used to desorb nonvolatile molecules that then undergo chemical ionization by collisions with conventional reagent ions prior to analysis in a magnetic sector instrument with differential pumping [3]. In 1989, LD/Cl experiments were reported employing a pulsed valve for reagent gas introduction in a Fourier transform mass spectrometer [4].

In this study we report a further simplification of LD/Cl by circumventing the external production of reagent ions. Elimination of high pressure source conditions and probe heating is achieved at the same time. Only a relatively simple experimental setup is required and sample preparation is straightforward.

* Corresponding author.

PII S1387-3806(98)14015-0

The reagent ions are provided by a concentrated organic salt solution that at the same time acts as a liquid matrix and assists desorption. The laser energy is absorbed by small, dark particulates suspended therein.

Such binary liquid/solid matrices have been shown to be a useful alternative to conventional solid matrix-assisted laser desorption/ionization (MALDI) matrices for the analysis of intermediate molecular weight substances [5–7]. Because the liquid phase does not generally have a UV chromophore, the laser energy is absorbed by the solid particulates and desorption occurs via rapid thermal evaporation of the liquid. Liquid mixtures consisting of a non-UV-absorbing primary compound and UV-absorbing molecules as matrices for MALDI have also been reported [8].

Conventional solid matrices must meet several requirements, including UV absorption, vacuum stability, solubility in common solvents, co-crystallization with the analyte molecules, and good desorption and ionization capabilities. Because the ionization mechanisms in solid-state MALDI are not yet fully understood, selection of new matrices is empirical rather than systematic. Requirements for liquid matrices are less stringent: solubility in common solvents, co-crystallization, and UV absorption as criteria for matrix selection can be neglected.

Although it is not clear yet whether two-phase MALDI involves solution-phase or gas-phase ionization or both, we recently showed that the gas-phase proton affinity (PA) of the molecules used as the liquid phase is strongly correlated with the protonation and deprotonation capabilities in two-phase MALDI [9]. For example, protonation of the peptide substance P is favored by use of glycerol (PA = 874 kJ/mol) and deprotonation is favored by use of diethanolamine (PA = 954 kJ/mol). In contrast to liquid matrices such as glycerol and diethanolamine, the matrices presented in this study are viscous salt solutions at ambient temperature and provide preformed reagent ions with known gas-phase proton affinities. Upon laser irradiation, both neutral and ionic species are liberated from the liquid matrix. The former assist desorption of neutral analyte, whereas the latter are available as chemical ionization agent in the dense region of the expanding plume. These ions are available immediately without any preceding processes.

Up to now, investigations concerning laser desorption/chemical ionization using salts were limited to studies on positive ions desorbed from the solid phase: Wood and Marshall used ammonium bromide for LD/Cl of aromatic hydrocarbons that were thought to be protonated by the NH_4^+ ion [10]. However, the efficiency of the proton transfer reaction was fairly poor. Silver nitrate LD/Cl by Kahr and Wilkins was used for the analysis of hydrocarbon polymers and silver-attached oligomer ion species were detected in high abundance [11]. Cl of perfluorinated polyethers (PFPE) was performed by Cromwell and co-workers by using transition metal ions such as CU^+ and Ni^+ [12]. In their studies, two pulsed lasers were employed: a low fluence laser for analyte desorption and a high fluence laser for metal ion formation.

A related approach is the use of co-matrices for enhancement of signal intensity and reproducibility. Among these are ammonium halides and organic ammonium salts that have been applied as co-matrices with conventional solid phase matrices for UV-MALDI mass spectrometry. For example, Cheng and Chan tested their use in MALDI mass spectrometry of oligonucleotides in negative ion mode [13]. They found that all ammonium halides investigated display significant enhancement effects on the signal intensity of intact molecular DNA homopolymer anions. The fluoride salt exhibited the greatest enhancement. Currie and Yates investigated the use of a variety of ammonium salts as co-matrices in MALDI mass spectrometry of oligodeoxynucleotides [14]. They found that many of the alkylammonium salts prevented macroscopic crystallization, in which cases no ions were observed. While the highly hygroscopic alkylammonium halides prevent crystallization, inorganic and other organic salts can be used as co-matrices for solid MALDI matrices. Citrate, tartrate, and oxalate ammonium salts were used in two-component matrix experiments performed by Zhu et al. [15]. The addition of ammonium citrate to a UV-absorbing MALDI matrix (1:1 molar ratio) was found to greatly enhance both positive and negative

ion signals from DNA molecules. Besides suppressing adducts of DNA-alkali ion, the ammonium salt is believed to have a protonation/deprotonation function for oligonucleotides, although the mechanism was not determined.

Hygroscopic tetrabutylammonium (TBA) salts were chosen here as the liquid component of a binary liquid/solid matrix because of their ability to form hydrates that melt around room temperature. Silicon particulates were chosen as the solid component because they do not give rise to any interfering negative ion peaks. Although graphite particulates were shown to be equally effective as energy transfer media [9], production of intense carbon-cluster anions makes them less useful for mass analysis in negative ion mode (see Fig. 3 in [9]).

2. Experimental

The experiments were carried out with a home-built 2 m linear time-of-flight mass spectrometer (TOF-MS). Typical mass resolution full width at half maximum (FWHM-definition) in laser desorption experiments was about $m/\Delta m = 220$ and $m/\Delta m = 110$ at mass 350 and 1350, respectively. The instrument base pressure was 5×10^{-7} mbar with a liquid nitrogen trap. Five minutes after sample introduction, this pressure was reached again. Desorption was performed by using a nitrogen laser (337 nm) with a pulse width of 3 ns (Laser Science Inc., VSL-337ND-T). Attenuation of the laser was achieved by using glass plates and an adjustable iris. Laser pulse energies were in the range of 15 to 60 μJ. Ions were accelerated to an energy of 25 kV by a static potential and detected with a microchannel plate detector. Mass spectra acquired consisted of a sum of typically 50 consecutive single spectra in order to enhance the signal-to-noise ratio. Silicon particulates (325 mesh, corresponding to 45 μm in diameter) and diethanolamine were purchased from Aldrich. Tetrabutylammonium salts were purchased from Fluka (TBA acetate, TBA benzoate, TBA bromide, TBA chloride, TBA cyanide, TBA fluoride trihydrate, TBA hydroxide 30-hydrate, TBA perchlorate). Substance P was purchased from Sigma. γ-cyclodextrin, adenosine-5′-monophosphate monohydrate and bombesin were purchased from Fluka. All chemicals were used without further purification.

High mass resolution experiments were conducted on a 4.7 Tesla Fourier transform ion cyclotron resonance (FT-ICR) mass spectrometer comprising a cylindrical ion cell. The instrument base pressure was below 10^{-8} mbar. For FT-ICR experiments, an Nd:YAG laser (Continuum, Minilite ML-10) operated at 355 nm was used for desorption.

3. Sample preparation

Matrix solutions were prepared by adding approximately 70% by volume of water to the salt crystals. Subsequently, an approximately equal volume of silicon particulates was added. These mixtures were then mechanically shaken for at least 15 minutes in order to obtain a homogeneous suspension. A volume of ca. 0.5 μl was applied to the sample holder and allowed to dry. As already reported by Dale and co-workers, best results were obtained if a "flat" surface was prepared prior to addition of the analyte solution [9]. It is therefore necessary that the slurry spreads evenly over the probe prior to evaporation of excess water. The result is a particulate/liquid matrix mixture with dry appearance. If the preparation looks wet, too much of the salt was used and hardly any signals can be obtained. All salts used form hydrates with melting points slightly above room temperature. For example, TBA hydroxide · $4H_2O$ has a melting point of 26°C [16]. The concentrated solutions used were found to be vacuum stable.

Analyte solutions were prepared as 10^{-3}–10^{-2} M solutions in water, methanol, water/methanol, or water/acetonitrile mixtures, and 0.5 μl was applied on top of the "dry" matrix. After evaporation of the solvent, the sample holder was introduced into the vacuum chamber.

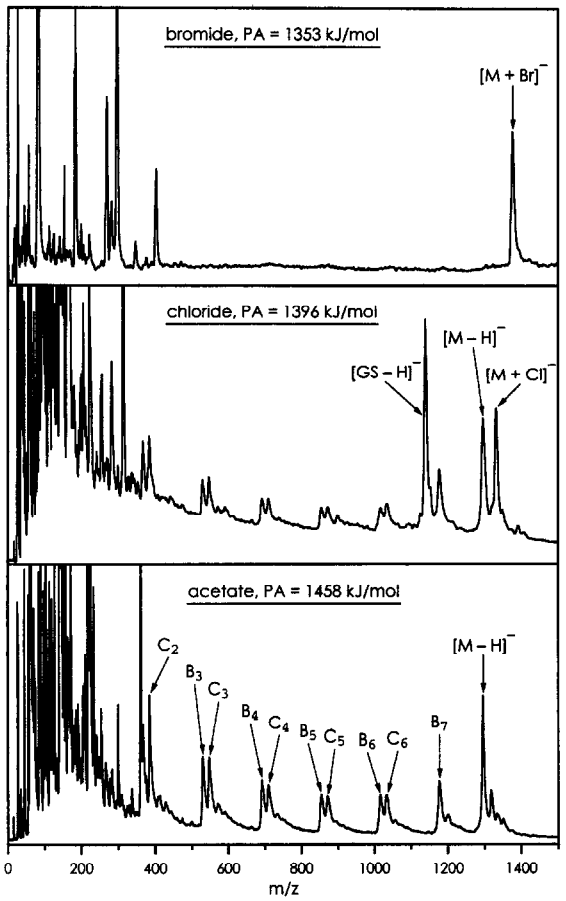

Fig. 1. Gamma-cyclodextrin (M) desorbed from various tetrabutylammonium salt matrices in negative ion mode. From top to bottom: bromide, chloride, and acetate salt. The bromide matrix provides molecular mass information, whereas the chloride and acetate matrices additionally provide structural information. The laser pulse energy was 55 μJ. In the middle trace, Gramicidin S (GS) was used as internal calibrant. B_x- and C_x-type series ions primarily differ in the fate of the glycosidic oxygen at the point of cleavage. In the B_x series, the oxygen remains on the neutral fragment, whereas in the C_x series it stays on the ionic fragment [18].

4. Results and discussion

Figure 1 shows spectra of γ-cyclodextrin desorbed from TBA bromide, TBA chloride, and TBA acetate matrices. The main types of ions observed with this method are illustrated: (a) quasimolecular ions formed by halide ion attachment, (b) deprotonated molecules, and (c) specific fragment ion species. The bromide salt can be used for molecular mass information, as it provides the $[M + Br]^-$ quasimolecular ion. Whereas the bromide ion forms a stable addition complex, the acetate salt yields deprotonated analyte ions. The chloride ion, with a PA in between that of bromide and acetate, forms both the addition complex and the deprotonated molecule plus fragment ions, but causes less intense fragmentation than acetate. By choice of the salt matrix, selective mass spectral information is obtained.

These results clearly show that the observed fragmentation is not a simple result of laser exposure. Since γ-cyclodextrin is not UV absorbing, photofragmentation can be excluded. Pyrolysis can also be excluded because no fragment ions were observed with the bromide matrix at the same laser pulse energy.

For comparison, neither a diethanolamine/silicon nor a glycerol/graphite binary matrix yielded any negative γ-cyclodextrin ion species, but an intense $[M + Na]^+$ signal. At elevated laser pulse energies, low abundance positive fragment ions were observed with glycerol/graphite [6], but spectral quality was decreased and the signal-to-noise ratio for the fragment ions was only about five. The observed fragment ions corresponded to successive cleavage of the γ-cyclodextrin at its glycosidic linkages and can be attributed to pyrolysis products. In the case of the TBA acetate matrix, pyrolysis effects do not seem to play a major role. Not only are more abundant fragment ions found, but also a different fragmentation pattern. In addition to the deprotonated molecule, an initial loss of 118 Da and further losses of 162 Da were observed. Moreover, a series of fragments starting with $[M–102–162]^-$ and subsequent losses of 162 Da was observed. This is similar to the pattern obtained under infrared laser desorption conditions in positive ion mode, where an initial loss of 102 Da from both sodiated and potassiated molecular ions is followed by further losses of 162 Da [17].

Spengler and co-workers suggest that the most prominent fragmentation pathway involves a series of retro-aldol reactions that are assumed to take place prior to ionization, in their case by attachment of an alkali-metal ion [17]. Although the $[M–102–H]^-$ ion

itself is not observed here, subsequent single sugar unit losses (Δm = 162 Da) are detected (indicated with C_x [18]). The series of $[M-118-x \cdot 162-H]^-$ ions (indicated with B_x [18]) can be explained by an additional loss of oxygen. These fragment ions only show up when using the TBA salt matrices with anion PAs higher than that of Br^-, but not when using the TBA bromide, diethanoleamine, or glycerol matrices.

Matrix ions were mainly detected as reagent anions (R^-), proton bound dimers of R^-, and $[(C_4H_9)_4NR + R]^-$ cluster ion species. The R^- ion was usually the most abundant. In the case of the fluoride and the hydroxide salts, the anticipated reagent anions could only be detected in minor or negligible amounts, whereas proton bound dimers ($[2F + H]^-$, $[20H + H]^-$) were the dominant peaks. $[(C_4H_9)_4NR + R]^-$ type ions are most likely created in the gas phase by reagent anion attachment to the matrix molecule. It is therefore fair to assume that besides the observed reagent anions, intact matrix molecules are also liberated during the desorption event. Cluster ions appear mostly at higher laser pulse energies (50–60 μJ) and can interfere with desirable fragment ions. However, these energies were only needed for desorption of relatively large molecules (MW > 1200 Da), and the mass range free of interference is still quite large (above 300–400 Da).

In the positive ion mode, the most prominent ion detected, even at elevated laser irradiance, is the $(C_4H_9)_4NR^+$ cation (*m/z* 242). This is occasionally accompanied by weak fragments at *m/z* 186 ($[(C_4H_9)_4N–C_4H_8]^+$) and *m/z* 142 ($[(C_4H_9)_4N–C_4H_8–C_3H_8]^+$). These results suggest that salt ions are generated during laser exposure by thermally induced dissociation. In no experiments were positive analyte ions observed.

In some, but not all cases, attachment of C_4H_8 to both the deprotonated molecule and deprotonated fragment ions was observed. It is known that larger alkyl homologs of tetramethylammonium fluoride decompose above 80°C [19]. The same should apply to tetrabutylammonium salts in general, so it is not surprising that alkyl fragments are generated under laser desorption conditions. These can then attach to either neutral or ionic species.

The observed ion types are expected to result from ion-molecule reactions similar to those in chemical ionization. Reagent anions of relatively low proton affinity such as chloride and bromide usually cannot react by proton transfer, but may form stable addition complexes as observed for γ-cyclodextrin with the TBA bromide matrix [20]

$$X^- + M \rightarrow MX^- \quad (1)$$

where X^- is the halide anion and M is the analyte molecule. With saccharose as analyte, the TBA chloride matrix yielded some $[M–H]^-$ ions, but formed mainly chloride adducts. Chloride addition complexes with saccharides from conventional Cl is also known [21]. The reaction leading to deprotonation of analyte molecules as observed for the γ-cyclodextrin/TBA acetate system is expected to be a proton transfer reaction:

$$R^- + M \rightarrow [M - H]^- + RH \quad (2)$$

where R^- stands for reagent anions. This type of reaction was shown to proceed in the gas phase with unit efficiency under equilibrium conditions, provided that the exoergicity of the reaction is at least 10 kcal/mol [22]. Fragment ions, the third type of observed species, are thought to be secondary products of deprotonation reactions with high exothermicity.

One general advantage of Cl as an ionization method is that the energy deposited into the analyte molecule has a well-defined upper limit given the enthalpy of the proton transfer reaction. Thus, unimolecular fragmentation can be controlled by choice of the reagent ion. Speir and Amster studied the fragmentation mechanisms of protonated peptide molecules generated by LD/Cl and found that although the internal energy of laser desorbed molecules has not yet been established quantitatively, the major contribution leading to fragmentation results from the Cl process rather than from desorption [23, 24]. In order to investigate the fragmentation behavior in deprotonation reactions with increasing exothermicity, adenosine-5′-monophosphate (AMP) was used as a probe. AMP is a relatively fragile molecule that yields specific fragment anions at *m/z* 79 (PO_3^-), *m/z* 97

($H_2PO_4^-$), *m/z* 134 (deprotonated adenine), and *m/z* 211 ([AMP–adenine–H]$^-$) under direct laser desorption conditions (248 nm). Besides an intense molecular ion, these fragments were also observed with the TBA salt matrices. Spectra of AMP desorbed from the TBA chloride and the TBA hydroxide matrices are shown in Fig. 2. The gas phase basicities and proton affinities of the selected anions are listed in Table 1.

Note the comparatively intense fragment ion signals yielded by the hydroxide matrix, whereas in the case of the chloride matrix the overall fragment ion intensity was much smaller. Mass spectra of AMP were recorded from the various TBA salt matrices. By using a constant laser pulse energy of 20 μJ, the normalized fragment ion abundance was found to increase systematically as the proton affinity of the reagent anion increases. Concurrently, the normalized molecular ion abundance decreased with increasing reagent anion proton affinity, as illustrated in Fig. 3. Although the bromide isotope at *m/z* 79 and the PO_3^- ion could not be resolved with our apparatus, the intensity of the latter was determined by calculating the ^{79}Br contribution from the ^{81}Br peak. The TBA perchlorate matrix did not yield any analyte ions under these conditions.

The [M–H]$^-$ product initially formed in reaction 2 clearly retains a large portion of the reaction energy that then enables fragmentation:

$$[M–H]^-* \rightarrow \text{fragments} \quad (3)$$

Fragmentation energies for AMP-related dinucleotides were measured to be in the range 80–100 kJ/mol, with activation energies of about 120 kJ/mol [27]. The proton affinity of [AMP–H]$^-$ can be estimated to lie between that of the bromide (1353 kJ/mol) and the perchlorate (1200 kJ/mol) anion because the TBA perchlorate did not yield an [AMP–H]$^-$ signal whereas the bromide matrix did. The proton affinity of the PO_3^- anion is 1300 kJ/mol which further suggests a PA of [AMP–H]$^-$ not greater than 1300 kJ/mol [25]. Assuming a PA of 1250 kJ/mol for the AMP anion, the maximum energy from deprotonation (PA(R^-)–PA([AMP–H]$^-$)) is greater than the activation energy for fragmentation for all reagents with a PA greater than that of bromide. For example, using acetate as reagent, the PA difference is about 208 kJ/mol.

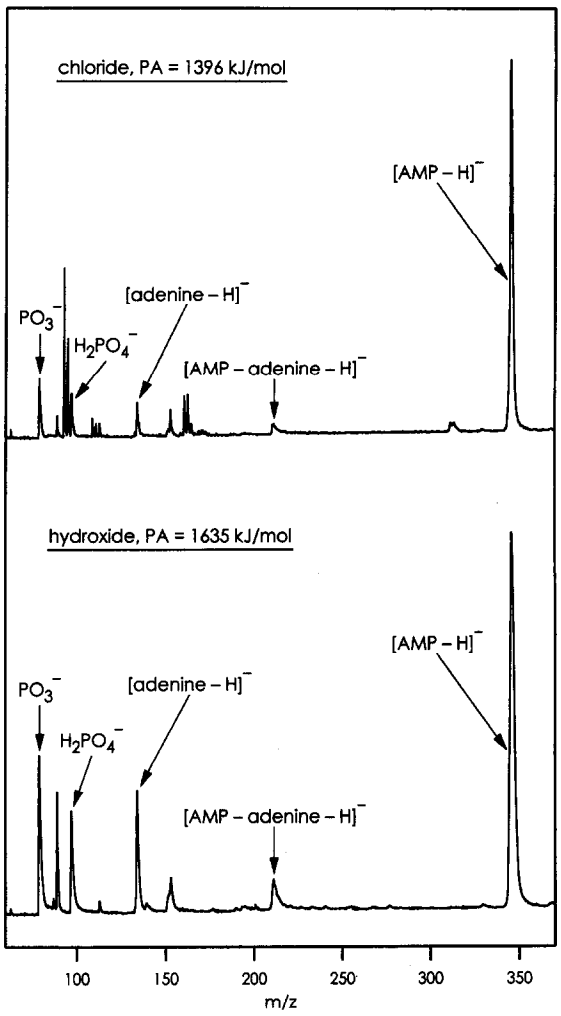

Fig. 2. Negative ion mode mass spectra of adenosine-5′-monophosphate (AMP) desorbed from tetrabutylammonium chloride matrix (upper trace) and tetrabutylammonium hydroxide matrix (lower trace). The higher PA of the hydroxide compared to the chloride matrix imparts elevated internal energy into the AMP molecule during ionization, resulting in enhanced specific fragmentation. Fragment ions can be assigned to phosphoric acid, adenine, and base loss. Peaks not annotated are matrix signals. The laser pulse energy was 20 μJ.

As is seen in Fig. 2, the [AMP–H]$^-$ ion decomposes via multiple fragmentation channels. Because the activation energies for these different channels are

Table 1
Proton affinities and gas phase basicities of the anions used

Anion	Proton affinity [kJ/mol]	Gas-phase basicity [kJ/mol]	Reference	Mass [Da]
OH^-	1634.7 ± 0.4	1607.1 ± 0.8	25	17
F^-	1553.5 ± 8.8	1529.7 ± 8.4	26	19
CN^-	1457.0 ± 8.4	1427.0 ± 8.8	25	26
CH_3COO^-	1457.5 ± 10.6	1428.0 ± 8.4	25	59
$C_6H_5CO_2^-$	1423.0 ± 9.2	1394.0 ± 8.4	25	121
Cl^-	1396.2 ± 8.8	1373.6 ± 8.4	26	35, 37
Br^-	1353.0 ± 8.8	1331.0 ± 8.4	25	79, 81
ClO_4^-	1300.0 ± 59.0	1180.0 ± 63.0	25	99,101

small compared to the enthalpy deposited by proton transfer and the variation among them is even smaller, we treat all activation energies as about equal (E_0). In this case, the total unimolecular dissociation rate constant, k_{uni}, can be expressed as the sum of the microscopic rate constants k_i for each channel [28]

$$k_{uni} = \sum_i k_i = \sum_i A_i \cdot \exp\left[\frac{-E_i}{k_B T}\right] \approx \exp\left[-\frac{E_0}{k_B T}\right] \cdot \sum_i A_i \quad (4)$$

Reaction (3) will be driven further toward fragments when greater excess enthalpy is deposited by the prior proton transfer step. Assuming that this energy is thermalized within the ions and neglecting the room temperature internal energy of $k_B T(300\ K) = 2.5$ kJ/mol, the enthalpy deposited by proton transfer gives the effective temperature of $[AMP–H]^-$ prior to fragmentation: $T_{eff} = \Delta H_{PT}/k_B$. It follows that

$$k_{uni} \propto \exp\left[-\frac{E_0}{\Delta H_{PT}}\right] \quad (5)$$

For first order unimolecular decay, the relative number of undissociated molecular ions at a given time t is

$$\frac{N(t)}{N_0} = \exp\left[-k_{uni} \cdot t\right] \quad (6)$$

Combining (4) through (6), we obtain

$$\frac{N(t)}{N_0} = \exp\left[-\exp\left(-\frac{E_0}{\Delta H_{PT}}\right) \cdot t \cdot \sum_i A_i\right] \quad (7)$$

where ΔH_{PT} is given by the difference in PA of reagent anion and deprotonated molecule [PA(R^-)–PA([AMP–H]$^-$)].

Because only ions formed within a short characteristic time after the laser desorption event will be focused on the detector of the mass spectrometer, Eq. (7) gives the observed relative $[AMP–H]^-$ abundance as a function of ΔH_{PT} at this time. Eq. (7) was fit to the data of Fig. 3. Within the experimental scatter, the fit is quite good. An $[AMP–H]^-$ proton affinity of 1279 kJ/mol was derived from the fit, corresponding well with the estimated value of 1250 kJ/mol. The E_0 value from the fit is 157 kJ/mol, also in good agreement with the estimated value of above 120 kJ/mol [27].

The amount of internal energy deposited into the analyte ions by LD/Cl can be varied in relatively small steps of about 50 kJ/mol. In principle, the step size for excess energy deposition can be decreased further by employment of additional bases. Increased internal energy shows an effect on the degree of fragmentation. However, the width of the internal energy distribution is not known. Because the reagent anions are liberated by a thermal desorption process, a relatively broad internal energy distribution cannot be excluded. An indication for this is given by the fact

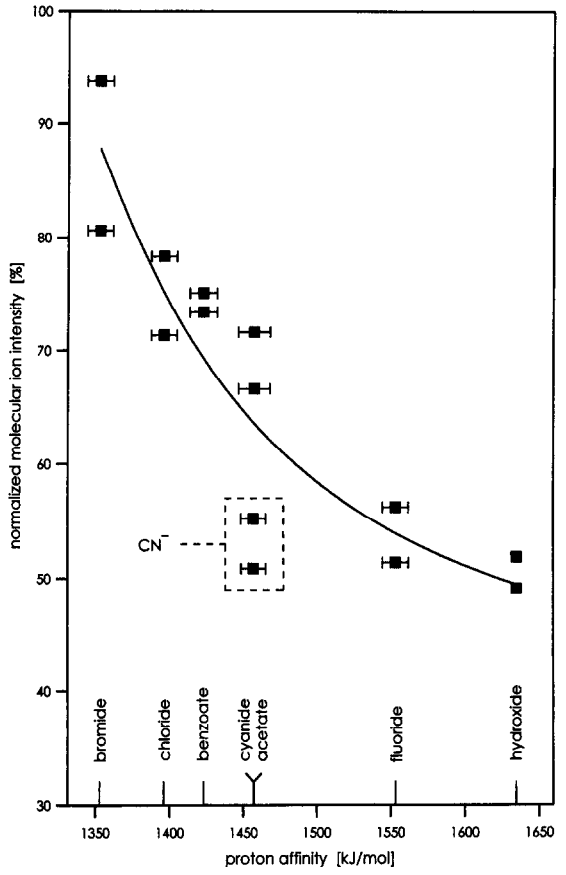

Fig. 3. Normalized molecular ion intensity of adenosine-5′-monophosphate (AMP), as a function of the reagent anion proton affinity. The normalized molecular ion intensity was calculated from the absolute molecular ion and fragment ion intensities, respectively, where the fragment ion intensity was determined by summing the integrals of the signals at m/z 79 (PO_3^-), m/z 97 ($H_2PO_4^-$), m/z 134 (deprotonated adenine), and m/z 211 ([AMP–adenine–H]$^-$). The relative molecular ion intensity correlates with the PA of the reagent anion used. The solid curve shows a fit function of the type (7). The laser pulse energy was 20 μJ. Data points surrounded by dashed lines are those obtained by use of the TBA cyanide matrix.

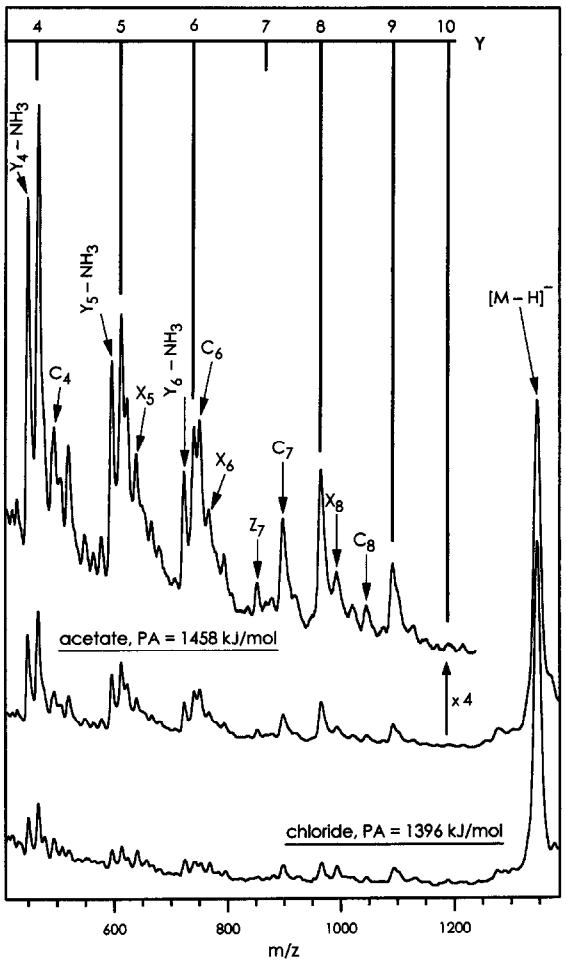

Fig. 4. Substance P (Arg-Pro-Lys-Pro-Gln-Gln-Phe-Phe-Gly-Leu-Met-NH_2) desorbed from a TBA acetate matrix (upper trace) and a TBA chloride matrix (lower trace), in negative ion mode. Useful structural information is obtained by controlled selective fragmentation of the peptide. The laser pulse energy was 40 μJ.

that the chloride anion forms both addition complexes and deprotonated sugar ion species.

A variety of peptides were investigated by using TBA salts in MALD/Cl: Phe-Gly-Gly-Phe, Val-Ala-Ala-Phe, $(Phe)_5$, $(Ala)_6$, $(Tyr)_6$, bombesin, substance P, and gramicidin S. All yielded intense signals of the deprotonated molecule by use of the TBA acetate matrix. $(Ala)_6$ and Val-Ala-Ala-Phe yielded spectra completely devoid of fragmentation. For the other peptides, fragment ions were also observed as depicted in Fig. 4. These can be assigned to deprotonated Y-, X-, C-, and Z-type fragments. These fragments do not appear in spectra obtained with a diethanoleamine matrix (see Fig. 2 in [9]). The TBA chloride matrix yielded a signal of deprotonated substance P, but fragmentation was observed to be less intense (see lower trace in Fig. 4).

A similar effect of matrix anion proton affinity on the degree of fragmentation was found for the peptide bombesin. Spectra of bombesin obtained by use of the

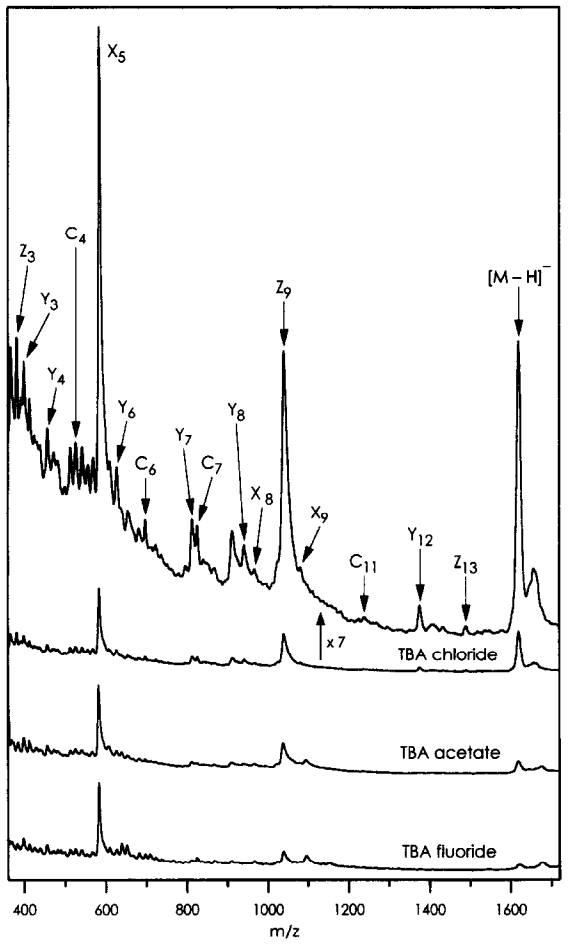

Fig. 5. Bombesin (pGlu-Gln-Arg-Leu-Gly-Asn-Gln-Trp-Ala-Val-Gly-His-Leu-Met-NH_2) desorbed from a tetrabutylammonium fluoride, acetate, and chloride matrix, in negative ion mode. The laser pulse energy was 60 μJ.

TBA chloride, acetate, and fluoride salt matrices are presented in Fig. 5. For comparison, spectra were normalized on the peak height of the X_5 signal. Just as in the case of γ-cyclodextrin, AMP, and substance P, fragmentation was found to increase as the proton affinity increases in the series $F^- > CH_3COO^- > Cl^-$. The hydroxide salt matrix did not give increased fragmentation compared to the fluoride salt matrix. However, the cyanide salt gave the same fragmentation as the fluoride and the hydroxide salt matrices, in contrast to what can be expected from its PA. The same effect was already observed with AMP as analyte, but we are not yet in a position to explain this effect. Spectra in Fig. 5 were obtained with 60 μJ laser pulse energy, and it should be noted here that for increasing analyte mass, increased laser pulse energies were required, as usual in two-phase MALDI [6].

Because the mass resolution in our time-of-flight (TOF) instrument was not sufficient to unambiguously assign ion signals in the higher mass region, reference experiments were carried out by using a Fourier-transform ion cyclotron resonance (FT-ICR) mass spectrometer. Isotopic profiles obtained by use of the salt matrices confirmed mass assignments of the $[M–H]^-$ peptide signals. In the FT-ICR mass spectrometer, the analyte signal was exhausted after about ten shots from the same sample position. We attribute this to dehydration of the liquid phase during the 30-min pumpdown in the FT-ICR mass spectrometer. In contrast, in the TOF mass spectrometer, where the pumpdown takes only a few minutes, ion signals were stable for up to several hundred shots.

In general, we observe mainly C-terminal peptide fragment ions, whereas Kaufmann and co-workers observe mainly N-terminal fragment ions in post-source decay (PSD) analysis of protonated peptides generated with MALDI [29]. This may give a hint about the site of protonation and deprotonation, respectively. Protonation is likely to occur at the terminal NH_2 group, therefore A-, B-, and C-type fragment ions can be expected. On the other hand, if deprotonation occurs at the C-terminus, X-, Y-, and Z-type fragment ions can be expected. However, substance P and bombesin are $CONH_2$ rather than COOH terminated and the site of deprotonation is more likely to be an acidic amino acid side chain.

Kaufmann and co-workers found that the choice of a solid matrix in MALDI/PSD analysis can influence the parent ion stability, but they attribute this effect to crystallization behavior rather than thermochemical matrix properties [30]. They further emphasize that the major part of the activation energy imparted to analyte ions stems from ion/neutral collisions occurring in the expanding plume of ions and neutrals. Moreover, the choice of a suitable solid matrix for specific analyte fragmentation, even on the longer timescale of PSD analysis, can only be made empir-

ically, because the ionization mechanism in MALDI is not yet understood.

Calculation of the absolute energy deposited into the analyte molecules by means of Cl requires thermochemical data on the analyte anions that are not available. Therefore, we use the proton affinities of deprotonated alpha-amino acids to make an estimate for the peptides. O'Hair and Bowie found values between 1385 kJ/mol (L-histidine) and 1431 kJ/mol (glycine) [31]. Proton affinities of the deprotonated amino acid side chains were estimated to lie in the range of 1439 to above 1632 kJ/mol [32]. At least for deprotonated peptide molecules the PA can be assumed to lie in the range between 1385 and 1431 kJ/mol, and therefore it is consistent with the data that even a relatively weak base such as the chloride anion (PA 1396.2 kJ/mol) is able to abstract a proton from a peptide molecule. Assuming a peptide anion PA of 1400 kJ/mol, excess energies ranging from 25 up to 240 kJ/mol can be imparted into the analyte ion by use of TBA benzoate and hydroxide matrix, respectively.

It is interesting to note that PSD analysis of cationized species was reported to be less efficient than PSD of protonated peptides; cationized ions were found to be much more stable [29]. We found that analytes that usually yield sodium and potassium adducts in positive ion mode (γ-cyclodextrin, maltotriose, valinomycin) can easily be deprotonated and yield abundant specific fragmentation patterns by use of the appropriate salt matrix. Moreover, the fragment ion yield can be adjusted without changing instrumental parameters by choice of the salt matrix, contrary to PSD measurements where acceleration field strength, final ion kinetic energy, and residual gases all influence the degree of fragmentation [30].

5. Conclusions and outlook

A simple, controlled, and efficient method for performing chemical ionization following laser desorption (MALD/Cl) has been developed. It is a straightforward technique yielding molecular weights and controlled fragmentation in a single step. The method was successfully applied to several classes of analytes. Fragmentation is controlled by taking advantage of the differing proton affinities of the reagent anions. Proton abstraction from the analyte molecules then makes differing amounts of energy available for unimolecular dissociation.

References

[1] M.S.B. Munson, F.H. Field, J. Am. Chem. Soc. 88 (1966) 2621.
[2] K.R. Jennings, in Gas Phase Ion Chemistry, 2, Academic, New York, 1979, p. 126.
[3] R.J. Cotter, Anal. Chem. 52 (1980) 1767.
[4] I.J. Amster, D.P. Land, J.C. Hemminger, R.T. McIver, Anal. Chem. 61 (1989) 184.
[5] J. Sunner, E. Dratz, Y.C. Chen, Anal. Chem. 67 (1995) 4335.
[6] M. Dale, R. Knochenmuss, R. Zenobi, Anal. Chem. 68 (1996) 3321.
[7] K. Tanaka, H. Waki, Y. Idao, S. Akita, Y. Yoshida, T. Yoshida, Rapid Commun. Mass Spectrom. 2 (1988) 151.
[8] D.S. Cornett, M.A. Duncan, I.J. Amster, Anal. Chem. 65 (1993) 2608.
[9] M. Dale, R. Knochenmuss, R. Zenobi, Rapid Commun. Mass Spectrom. 11 (1997) 136.
[10] T.D. Wood, A.G. Marshall, J. Am. Soc. Mass Spectrom. 2 (1991) 299.
[11] M.S. Kahr, C.L. Wilkins, J. Am. Soc. Mass Spectrom. 4 (1993) 453.
[12] E.F. Cromwell, K. Reihs, M.S. de Vries, S. Ghaderi, H.R. Wendt, H.E. Hunziker, J. Phys. Chem. 97 (1993) 4720.
[13] S. Cheng, T.W.D. Chan, Rapid Commun. Mass Spectrom. 10 (1996) 907.
[14] G.J. Currie, J.R. Yates, III, J. Am. Soc. Mass Spectrom. 4 (1993) 955.
[15] Y.F. Zhu, N.I. Taranenko, S.L. Allmann, S.A. Martin, L. Haff, Rapid Commun. Mass Spectrom. 10 (1996) 1591.
[16] Fowler et al., J. Am. Chem. Soc. 62 (1940) 1141.
[17] B. Spengler, J.W. Dolce, R.J. Cotter, Anal. Chem. 62 (1990) 1731.
[18] B. Domon, C.E. Costello, Glycoconjugate J. 5 (1988) 397.
[19] J.H. Clark, Chem. Rev. 80 (1980) 429.
[20] J.R. Chapman, Practical Organic Mass Spectrometry: A guide for chemical and biochemical analysis, 2nd ed., Wiley, West Sussex, England, 1993.
[21] A.K. Ganguly, N.F. Cappucino, H. Fujiwara, and A.K. Bose, J. Chem. Soc. Chem. Commun. (1979) 148.
[22] D.K. Bohme, Ion chemistry: A new perspective, Trans. R. Soc. Can., Ser. IV, XIX (1981) 265.
[23] J.P. Speir and I.J. Amster, J. Am. Soc. Mass Spectrom. 6 (1995) 1069.
[24] J.P. Speir, G.S. Gorman, D.S. Cornett, I.J. Amster, Anal. Chem. 63 (1991) 65.
[25] M.T. Rogers, S. Campbell, E.M. Marzluff, and J.L.

Beauchamp, Int. J. Mass Spectrom. Ion Processes 137 (1994) 121.

[26] J.E. Bartmess, "Negative Ion Energetics Data" in NIST Standard Reference Database Number 69, W.G. Mallard, P.J. Linstrom (Eds.), August 1997, National Institute of Standards and Technology, Gaithersburg, MD 20899 (http://webbook.nist.gov).

[27] G.L. Lias, J.E. Bartmess, J.F. Liebman, J.L. Holmes, R.D. Levin, W.G. Mallard, J. Phys. Chem. Ref. Data 17, Suppl. 1, 1988.

[28] R.G. Gilbert, S.C. Smith, Theory of Unimolecular and Recombination Reactions, Physical Chemistry Texts, Blackwell Scientific, 1990.

[29] R. Kaufmann, B. Spengler, F. Lützenkirchen, Rapid Commun. Mass Spectrom. 7 (1993) 902.

[30] B. Spengler, D. Kirsch, R. Kaufmann, J. Phys. Chem. 96 (1992) 9678.

[31] R.A.J. O'Hair, J.H. Bowie, S. Gronert, Int. J. Mass Spectrom. Ion Processes 117 (1992) 23.

[32] E.M. Marzluff, S. Campbell, M.T. Rogers, J.L. Beauchamp, J. Am. Chem. Soc. 116 (1994) 7787.